

Electronic Supplementary Information for

One-pot synthesis of mercapto functionalized Zr-MOFs  
for the enhanced removal of Hg<sup>2+</sup> ions from water

Daiwu Lin,<sup>‡a</sup> Xiao Liu,<sup>‡a</sup> Renliang Huang,<sup>\*b</sup> Wei Qi,<sup>\*ac</sup> Rongxin Su,<sup>ac</sup>

Zhimin He <sup>a</sup>

<sup>a</sup> State Key Laboratory of Chemical Engineering, School of Chemical Engineering  
and Technology, Tianjin University, Tianjin 300072, P.R. China

<sup>b</sup> Tianjin Key Laboratory of Indoor Air Environmental Quality Control, School of  
Environmental Science and Engineering, Tianjin University, Tianjin 300072, P.R.  
China

<sup>c</sup> Collaborative Innovation Center of Chemical Science and Engineering (Tianjin),  
Tianjin Key Laboratory of Membrane Science and Desalination Technology, Tianjin  
University, Tianjin 300072, P.R. China

---

\* Author to whom correspondence should be addressed:

tjuhrl@tju.edu.cn (R.H.), qiwei@tju.edu.cn (W.Q.)

<sup>‡</sup> Daiwu Lin and Xiao Liu contributed equally to this work.

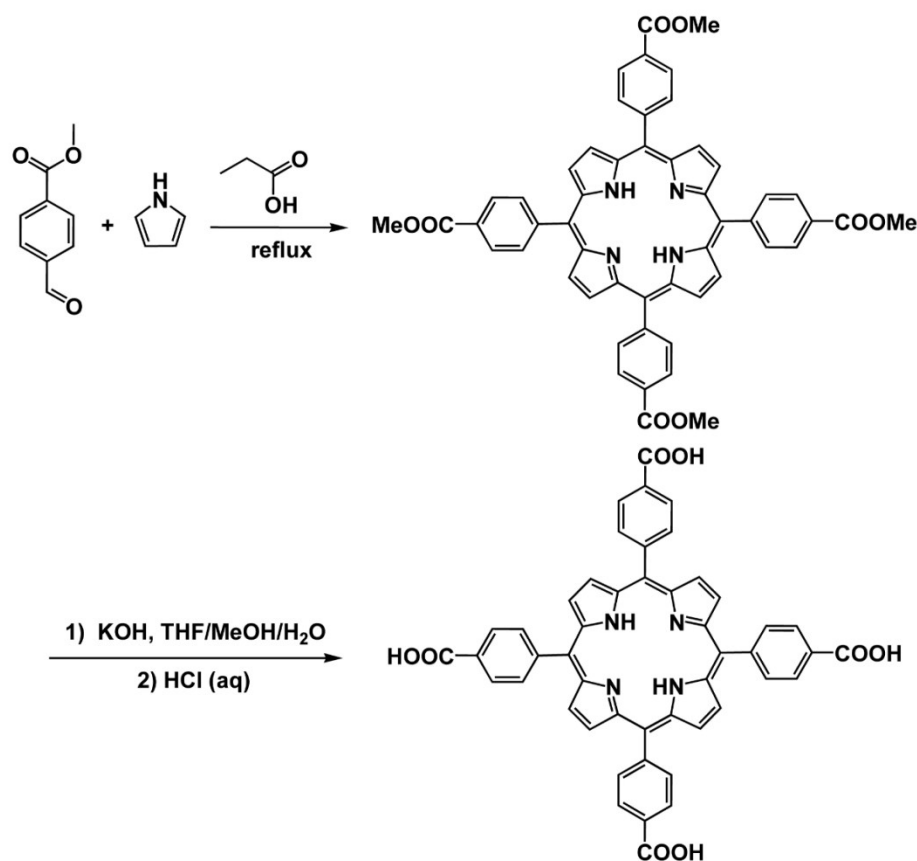
# 1. Materials and Methods

## 1.1 Materials

Mercury standard solution (1000 mg/L, 2% HNO<sub>3</sub>) was purchased from ANPEL Laboratory Technologies Inc. (Shanghai, China). Pyrrole, methyl *p*-formylbenzoate, propionic acid, zirconium chloride (ZrCl<sub>4</sub>), *N,N'*-dimethylformamide (DMF), benzoic acid (BA), mercaptoacetic acid (MAA) and alpha lipoic acid (ALA) were purchased from Aladdin Reagent Company (Shanghai, China). All chemicals are used without further purification.

## 1.2 Preparation of H<sub>2</sub>TCPP ligands

The H<sub>2</sub>TCPP ligand was synthesized based on previous reports with modifications.<sup>1</sup> Typically, the synthesis steps were as follows:



Scheme S1 Synthesis strategy for H<sub>2</sub>TCPP ligands.

### (1) 5,10,15,20-Tetrakis(4-methoxycarbonylphenyl)porphyrin (TPPCOOMe)

13.8 g methyl *p*-formylbenzoate was first dissolved in 200 mL of propionic acid, and then 6 g pyrrole was added dropwise before refluxing at 140 °C for 12 h in darkness.

Dark purple crystals were harvested by suction filtration with ethanol, ethyl acetate and THF washed, and dried under vacuum for 24 h.

## **(2) meso-Tetra(4-carboxyphenyl)porphine (H<sub>2</sub>TCPP)**

1.5 g TPPCOOMe was stirred in 50 ml of THF and 50 ml of MeOH mixed solvent, and then 50 mL of KOH solution with concentration of 2 mol/L was added before refluxing for 12 h. Residual THF and MeOH were evaporated by Rotary Evaporator after the reaction was completed, and the crude product was heated to dissolve with a little additional water added. The dissolved solution was acidized with hydrochloric acid until no further precipitate was produced. Note that too much HCl would result in the formation of undesired green solid. Finally, the solid was harvested by filtration, washed with water for several times and dried under vacuum.

### **1.3 One-pot synthesis of mercapto functionalized Zr-MOFs**

For PCN-222-MAA(O), 25 mg ZrCl<sub>4</sub>, 25 mg H<sub>2</sub>TCPP, and 340 μL MAA were dissolved in 3 mL of DMF. For PCN-224-MAA(O), 100 mg ZrCl<sub>4</sub>, 10 mg H<sub>2</sub>TCPP, and 340 μL MAA were dissolved in 3 mL of DMF. For PCN-224-ALA(O), 50 mg ZrCl<sub>4</sub>, 10 mg H<sub>2</sub>TCPP, and 500 mg ALA were dissolved in 3 mL of DMF. All the resulting mixture was heated at 120 °C for 24 h. After cooling to room temperature, the mercapto functionalized Zr-MOFs (PCN-222-MAA(O), PCN-224-MAA(O), or PCN-224-ALA(O)) were harvested by centrifugation, washing with DMF and methanol each three times, and dried in vacuum oven.

### **1.4 Synthesis of mercapto functionalized Zr-MOFs via postsynthetic modification**

PCN-222 and PCN-224 were synthesized according to the reported literature.<sup>2, 3</sup> For PCN-222, 50 mg ZrCl<sub>4</sub>, 50 mg H<sub>2</sub>TCPP and 2.7 g benzoic acid were ultrasonically dissolved in 8 mL of DMF. The mixture was heated at 120 °C for 2 days and then at 130 °C for 1 day. For PCN-224, 30 mg ZrCl<sub>4</sub>, 10 mg H<sub>2</sub>TCPP and 400 mg benzoic acid were ultrasonically dissolved in 2 mL of DMF. The mixture was heated at 120 °C for

24 h. After cooling to room temperature, the PCN-222 or PCN-224 crystals were harvested by suction filtration with DMF and methanol washed each three times.

To activate the samples, the as-synthesized PCN-222 or PCN-224 was suspended in 80 mL of DMF and 1.5 mL of the concentrated HCl mixed solution followed by stirring at 120 °C for 12 h. Finally, the activated samples were centrifuged and washed with DMF and acetone each three time, and dried under vacuum.

30 mg of the activated PCN-222 or PCN-224, 30  $\mu$ L mercaptoacetic acid or 50 mg alpha lipoic acid were dissolved in 3 mL of DMF. The mixture was heated at 120 °C for 24 h. After cooling to room temperature, the mercapto functionalized Zr-MOFs (PCN-222-MAA(P), PCN-224-MAA(P), or PCN-224-ALA(P)) were harvested followed by centrifugation, washing with DMF and methanol each three times, and dried in vacuum oven.

### **1.5 Chemical stability and thermal stability**

25 mg of PCN-224-MAA(O) were suspended in 10 mL of aqueous solutions containing 1M HCl, or 10 mL of aqueous solutions with pH value of 1, 2, 6, 10, or 11, for 24 h. After treatment, the PCN-224-MAA(O) was collected for XRD analysis.

For thermal stability, 5 mg of PCN-224-MAA(O) were heated on a thermal gravimetric analyzer (TGA, STA449F5), from 25 °C to 500 °C at a rate of 10 °C  $\text{min}^{-1}$  under 20 mL  $\text{min}^{-1}$  of  $\text{N}_2$ .

### **1.6 Adsorption performance assessment**

All the adsorption experiments were carried out at 25 °C and pH 6.0 unless otherwise noted. 2 mg of the original or the mercapto functionalized PCN-222 (PCN-224) was added to 20 mL of  $\text{Hg}^{2+}$  solution with an initial concentration of 100 mg/L. The resulting mixture was stirred at 1200 rpm for 12 h and then centrifuged at 12000 rpm for 10 min. The supernatants were collected for the determination of  $\text{Hg}^{2+}$  ions.

For the selectivity experiment, 10 mg PCN-224-MAA(O) was added to 10 mL of the mixture solution (pH 3.0) with eight heavy metal ions ( $\text{Hg}^{2+}$ ,  $\text{Cu}^{2+}$ ,  $\text{Cd}^{2+}$ ,  $\text{Co}^{2+}$ ,  $\text{Cr}^{3+}$ ,  $\text{Mn}^{2+}$ ,  $\text{Ni}^{2+}$ ,  $\text{Pb}^{2+}$ ). The initial concentration of each heavy metal ions was 100 mg/L.

The resulting mixture was stirred at 1200 rpm for 12 h and then centrifuged at 12000 rpm for 10 min. The supernatants were collected for the ICP-OES measurement.

The effect of pH value on adsorption of  $\text{Hg}^{2+}$  was investigated. 2 mg PCN-224-MAA(O) was added to 10 mL of 20 mg/L  $\text{Hg}^{2+}$  solution with the pH value from 2 to 8. The resulting mixture was stirred at 1200 rpm for 12 h and then centrifuged at 12000 rpm for 10 min. The supernatants were collected for the determination of  $\text{Hg}^{2+}$  ions.

The adsorption isotherm experiments were operated. 2 mg PCN-224-MAA(O) was added to 10 mL of  $\text{Hg}^{2+}$  solutions with different concentrations from 8.5 mg/L to 260 mg/L. The resulting mixture was stirred at 1200 rpm for 12 h and then centrifuged at 12000 rpm for 10 min. The supernatants were collected for the determination of  $\text{Hg}^{2+}$  ions.

The recycling and reuse of the PCN-224-MAA(O) was evaluated by adding 2 mg PCN-224-MAA(O) into 10 mL of 250 mg/L  $\text{Hg}^{2+}$  solution. The resulting mixture was stirred at 1200 rpm for 12 h and then centrifuged at 12000 rpm for 10 min. The PCN-224-MAA(O) was collected and then added to 10 mL of mixture solution of HCl (0.01 M) and thiourea (0.1%, wt). The resulting mixture was stirred at 1200 rpm for 1 h and then centrifuged at 12000 rpm for 10 min. Afterwards, the collected PCN-224-MAA(O) was washed with deionized water twice for next cycle.

## 1.7 Characterization

The concentrations of metal ions were determined by inductively coupled plasma optical emission spectrometer (ICP-OES, Thermo Scientific, 7000Series).<sup>4, 5</sup> For  $\text{Hg}^{2+}$  ions, the concentration gradient of the standard curve determined by ICP-OES was set as 1, 2, 5, 10, 20 mg/L, and the linear fitting curve was shown in Fig. S1. The concentrations of  $\text{Hg}^{2+}$  at low concentrations was measured by cold vapor atomic fluorescence spectrometer (CVAFS, Tekran 2500). The morphologies of the as-synthesized Zr-MOFs were observed by scanning electron microscope (Hitachi, S-4800). Powder X-ray diffraction (PXRD) patterns were obtained by X-ray diffractometer (Bruker, D8 advance) with Cu target. Fourier transform infrared (FTIR)

spectra were recorded by FTIR spectrometer (American Nicolet Corp., 6700) with a wavenumber range of 400-4000  $\text{cm}^{-1}$ . The UV-vis absorbance spectra were collected on a UV-vis spectrophotometer (Purkinje General, TU-1810). The weight loss of mercapto functionalized MOFs was analyzed by thermal gravimetric analyzer (TGA, STA449F5) with 5 mg sample in  $\text{Al}_2\text{O}_3$  crucibles. X-ray photoelectron spectroscopy (XPS, ESCALAB 250xi) was operated to investigate the interaction mechanism between Zr-MOFs-SH and  $\text{Hg}^{2+}$ .

## 2. Supplementary Results and Discussion

### 2.1 Adsorption kinetics

As shown in Fig. S13a, the concentration of  $\text{Hg}^{2+}$  ions significantly decreased upon the addition of PCN-224-MAA(O) and reached near zero after 10 min of adsorption, indicating that the PCN-224-MAA(O) exhibited a high adsorption rate.

The experimental data was demonstrated with pseudo-second-order kinetic model shown as equation (S1)<sup>6</sup>:

$$\frac{t}{q_t} = \frac{1}{K_2 q_e^2} + \frac{t}{q_e} \quad (\text{S1})$$

where  $q_t$  (mg/g) and  $q_e$  (mg/g) are the adsorption amount at time  $t$  (min) and at equilibrium, respectively.  $K_2$  (g/mg/min) is the rate constant of pseudo-second-order adsorption. As shown in Fig. S13b and Table S2, a high correlation coefficient of 0.9999 was obtained from the fitting with pseudo-second-order kinetics model, which indicated there was significant linear correlation between time ( $t$ ) and  $t/q_t$ . Furthermore, the  $q_e$  value calculated by equation (S1) was 71.9 mg/g, which is in agreement with the measured value (71.8 mg/g), suggesting that the adsorption kinetic of  $\text{Hg}^{2+}$  over PCN-224-MAA(O) follows the pseudo-second-order kinetic model.

### 2.2 Adsorption isotherms

To investigate the adsorption ability of PCN-224-MAA(O), the adsorption equilibrium isotherm of PCN-224-MAA(O) was determined and the results are presented in Fig. S14. With increasing the initial concentration of  $\text{Hg}^{2+}$  ions, the adsorbed amount of  $\text{Hg}^{2+}$  ions increased and then flattened out due to the saturation of adsorption. To describe adsorption isotherm, the equilibrium data of the adsorption

amounts was fitted by Langmuir model. The adsorption capacity of PCN-224-MAA(O) was calculated by the following equation (S2):

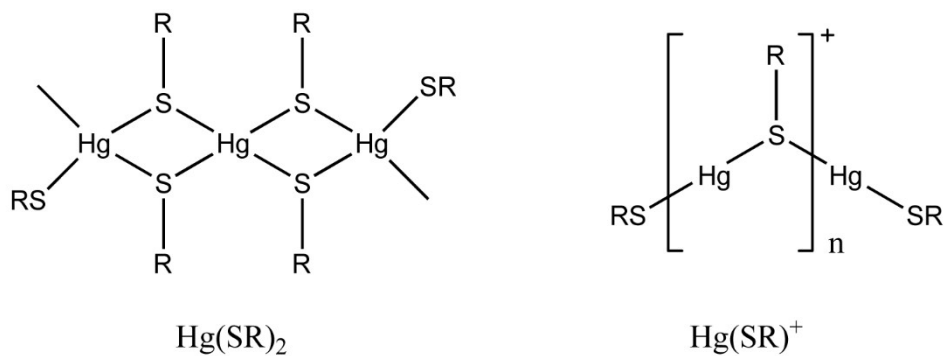
$$\frac{c_e}{q_e} = \frac{1}{K_L q_m} + \frac{c_e}{q_m} \quad (\text{S2})$$

where  $c_e$  (mg/L) is the equilibrium concentration;  $q_e$  (mg/g) and  $q_m$  (mg/g) are the equilibrium adsorption capacity and maximum adsorption capacity, respectively;  $K_L$  (L/mg) is Langmuir constant.

Equilibrium parameters are presented in Table S3. The correlation coefficient fitting by Langmuir model is up to 0.9992, indicating the adsorption of  $\text{Hg}^{2+}$  on PCN-224-MAA(O) was fitted well with Langmuir model. The Langmuir adsorption is considered to be a chemical adsorption with higher capacity and stability than simple physical adsorption, which could account for the fast and large adsorption capacity of  $\text{Hg}^{2+}$  onto mercapto modified Zr-MOFs. The maximum adsorption capacity of PCN-224-MAA(O) for  $\text{Hg}^{2+}$  ions is calculated to be 909.1 mg/g, and it's in accordance with the experimental value of 843.6 mg/g. In comparison with many other MOFs, PCN-224-MAA(O) had a higher adsorption capacity (Table S4).



### 3. Supplementary Figures



**Scheme S2** Diagram of coordination forms between  $\text{Hg}^{2+}$  and mercapto molecules.

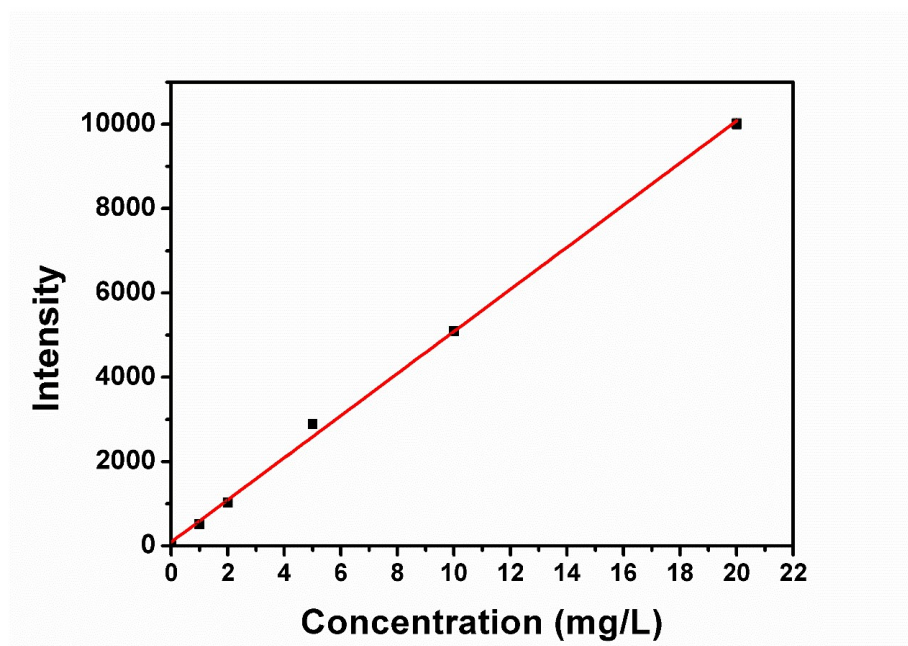


**Fig. S1** Standard curve of  $\text{Hg}^{2+}$  ions by ICP-OES (The linear correlation coefficient is 0.998).

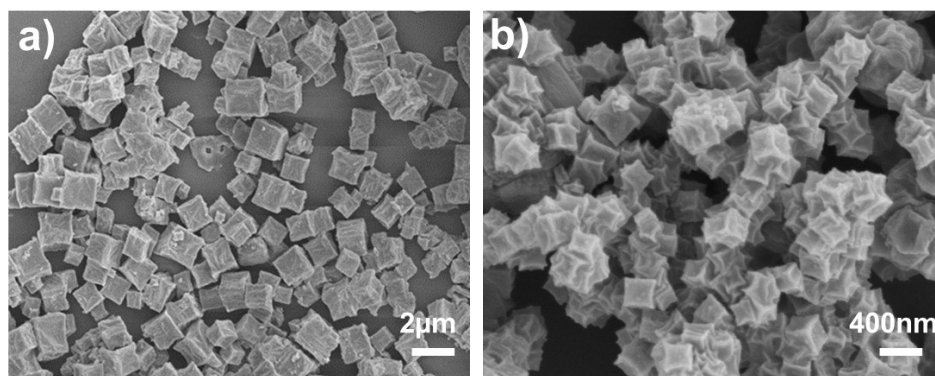


**Fig. S2** SEM images of a) PCN-224-ALA(P) and b) PCN-224-ALA(O).

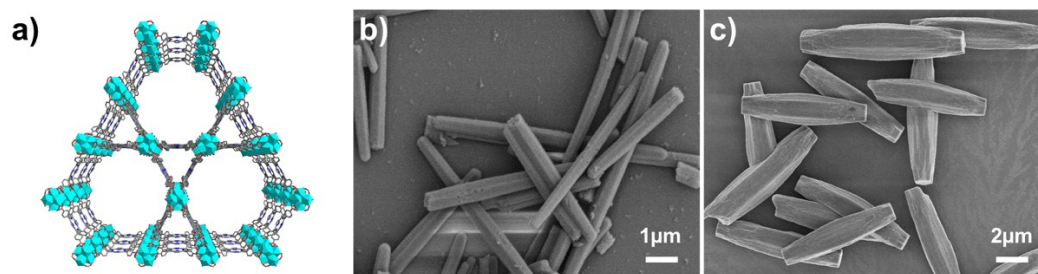


**Fig. S3** a) Crystal structure of PCN-222; b-c) SEM images of b) PCN-222-MAA(P) and c) PCN-222-MAA(O).

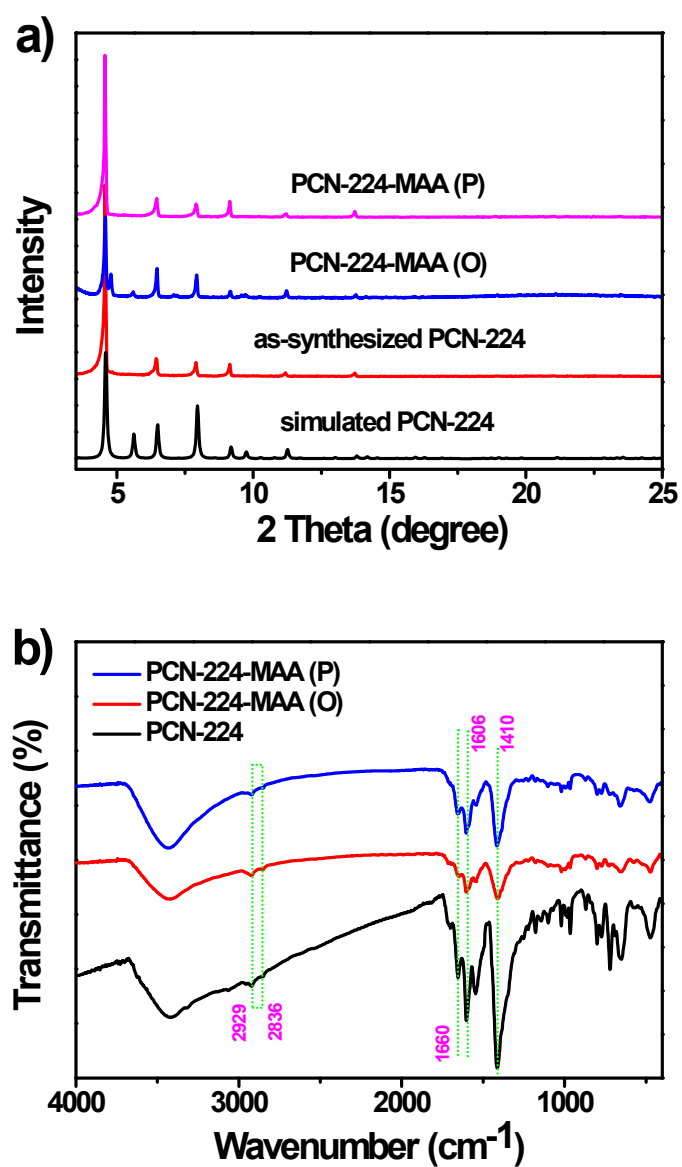


**Fig. S4** a) XRD patterns and b) FT-IR spectra of as-synthesized PCN-224, PCN-224-MAA(P) and PCN-224-MAA(O).

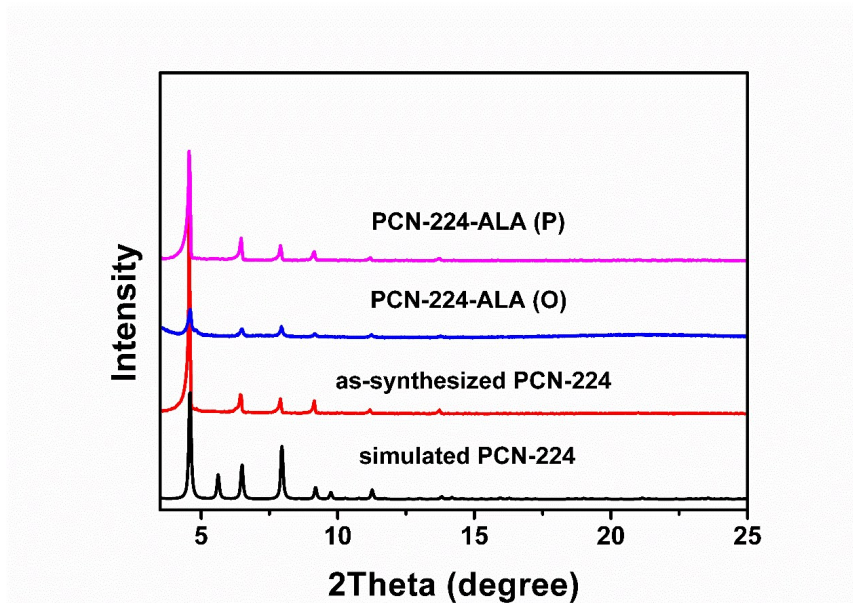


Fig. S5 XRD patterns of as-synthesized PCN-224, PCN-224-ALA(P) and PCN-224-ALA(O).

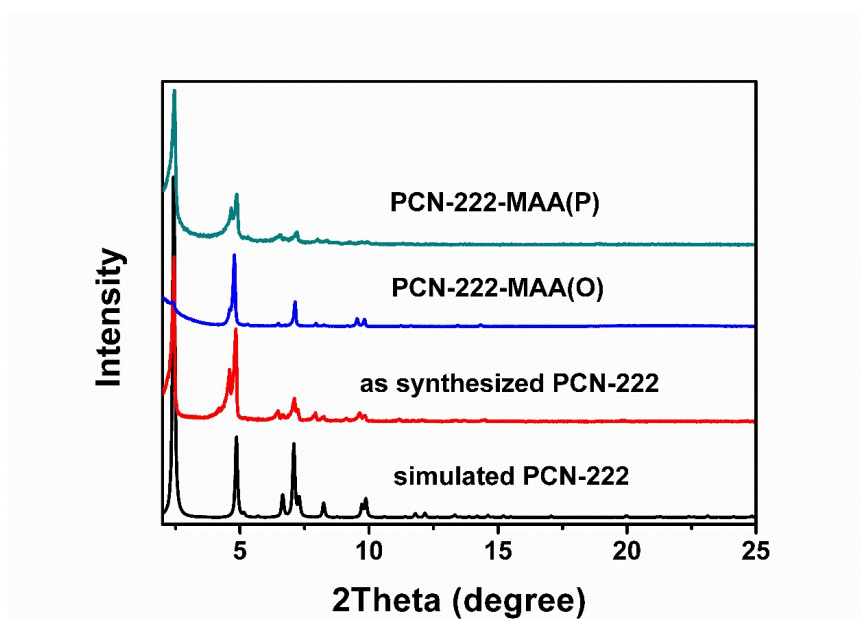


Fig. S6 XRD patterns of as-synthesized PCN-222, PCN-222-MAA(P) and PCN-222-MAA(O).

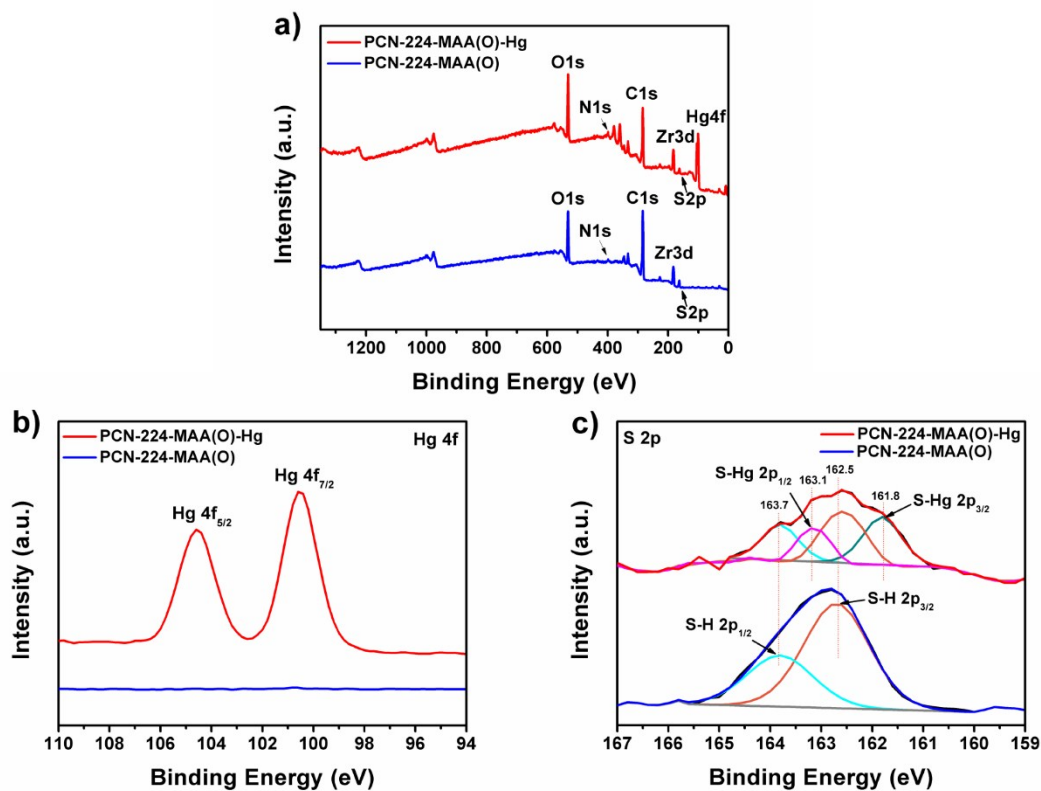


Fig. S7 XPS characterization of PCN-224-MAA(O) before and after the adsorption of Hg<sup>2+</sup>.

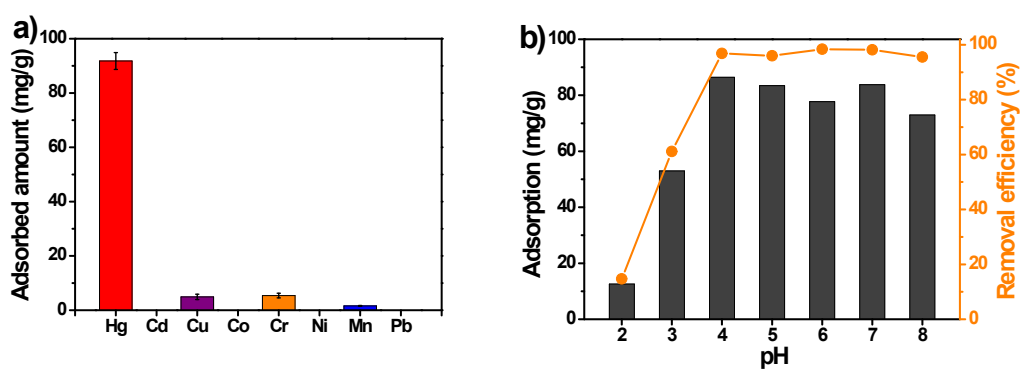


Fig. S8 a) Adsorption of mixed heavy metal ions (the concentration of each ions was 100 mg/L) on PCN-224-MAA(O) at pH 3. b) The effect of pH on the adsorption of Hg<sup>2+</sup> ions with an initial concentration of 20 mg/L on PCN-224-MAA(O).

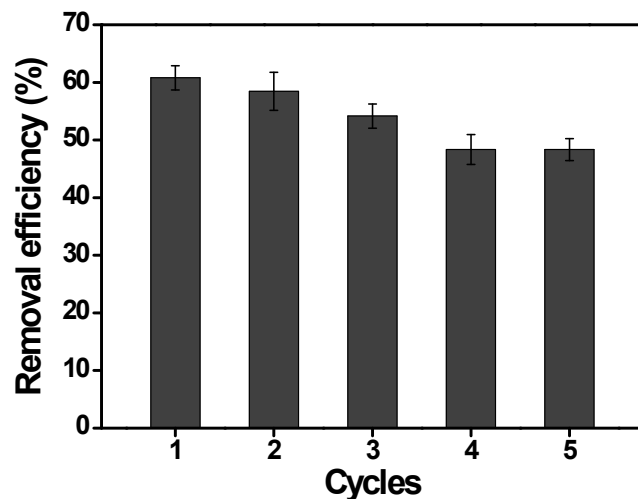


Fig. S9 The removal efficiency of  $\text{Hg}^{2+}$  ions in each cycle.

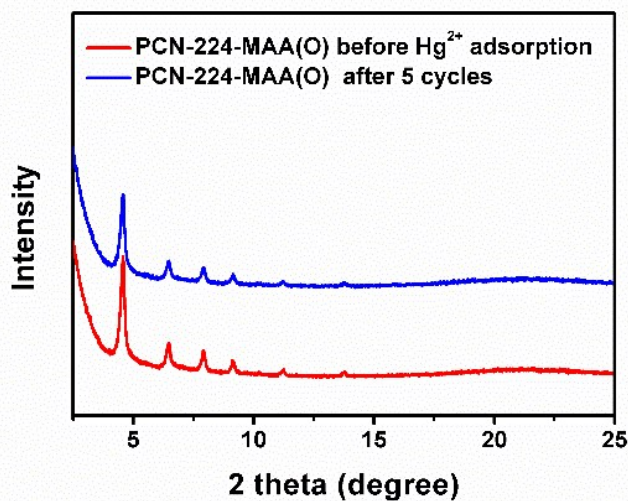


Fig. S10 XRD patterns of PCN-224-MAA(O) before  $\text{Hg}^{2+}$  adsorption and after 5 cycles reuse.

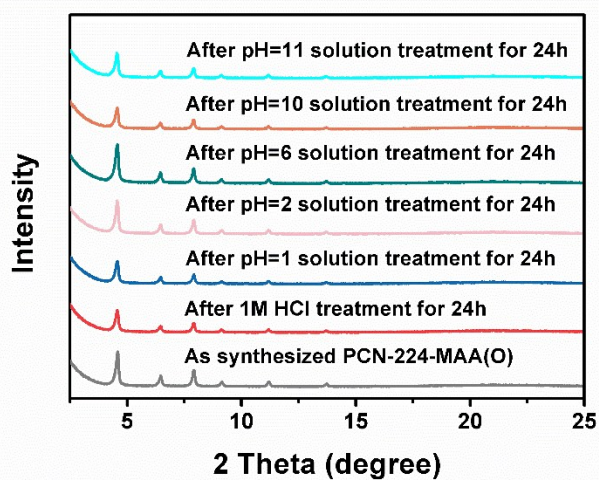


Fig. S11 XRD patterns of PCN-224-MAA(O) after acid or alkali treatment

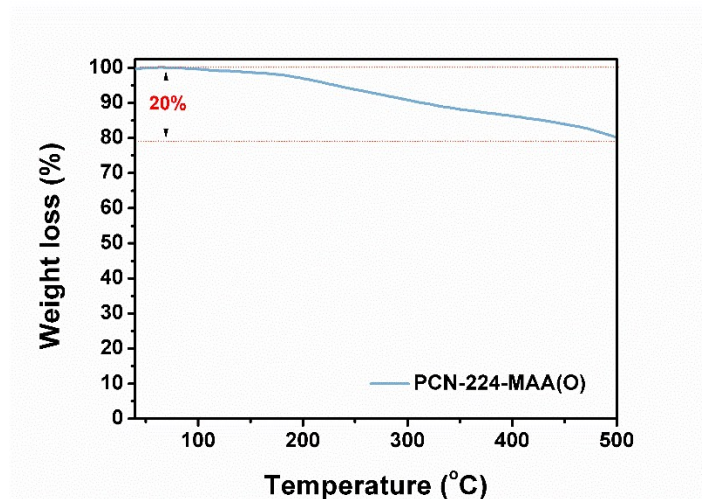


Fig. S12 Thermogravimetric analysis thermogram of PCN-224-MAA(O).

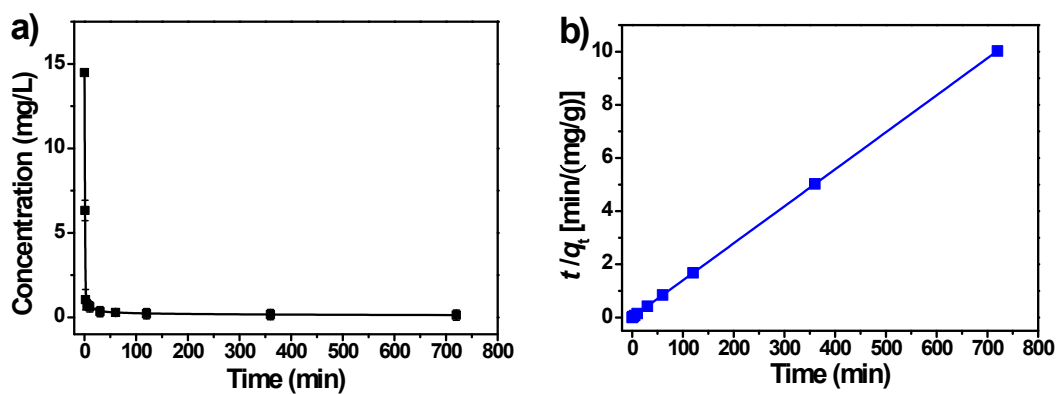
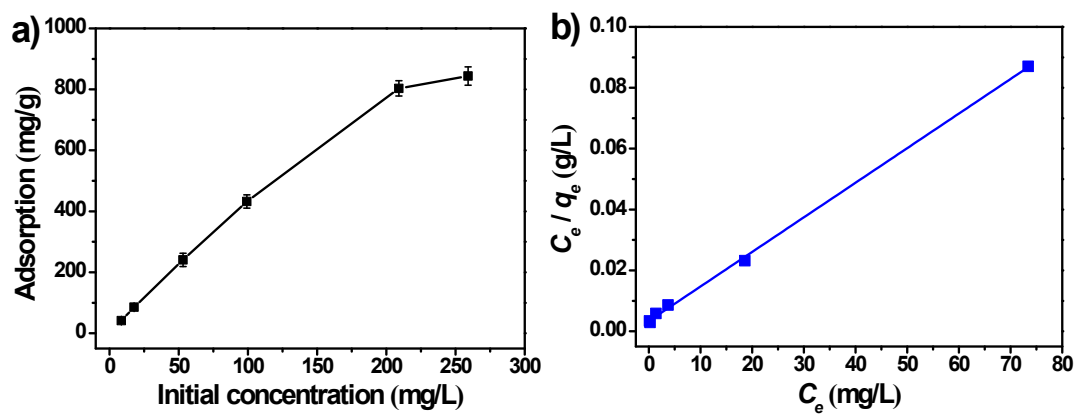


Fig. S13 a) The change in  $\text{Hg}^{2+}$  ions concentrations with the adsorption time; b) The pseudo-second-order kinetic plot for the adsorption of  $\text{Hg}^{2+}$  ions over PCN-224-MAA(O). The adsorption experimental conditions: 2 mg PCN-224-MAA(O), 10 mL  $\text{Hg}^{2+}$  solution, 20 mg/L initial  $\text{Hg}^{2+}$  concentration, pH 6.0, 25 °C.



**Fig. S14** a) Adsorption amount of Hg<sup>2+</sup> ions over PCN-224-MAA(O) at different initial concentrations of Hg<sup>2+</sup> ions; b) The linear regression by fitting the equilibrium adsorption data with Langmuir adsorption model.

## 4. Supplementary Tables

**Table S1** The content of mercapto groups and the adsorption capacity of  $\text{Hg}^{2+}$  ions ( $q$ ) in functionalized Zr-MOFs

	One-pot synthesis			Postsynthetic modification		
	PCN-224- MAA(O)	PCN-224- ALA(O)	PCN-222- MAA(O)	PCN-224- MAA(P)	PCN- 224- ALA(P)	PCN-222- MAA(P)
<b>SH</b> (mmol/g)	6.32	2.62	3.66	1.05	1.27	0.73
<b><math>q</math></b> (mg/g)	843.6	343.8	509.1	138.5	191.7	113.3

**Table S2** The parameters of pseudo-second-order kinetic model for  $\text{Hg}^{2+}$  adsorption

Metal ion	$q_e$ (exp) (mg/g)	Pseudo-second-order kinetic		
		$q_e$ (mg/g)	$K_2$ (g/mg/min)	$R^2$
$\text{Hg}^{2+}$	71.8	71.9	0.0317	0.9999

**Table S3** Equilibrium parameters of Langmuir adsorption model for  $\text{Hg}^{2+}$  adsorption

Metal ion	$q_e$ (exp) (mg/g)	Langmuir adsorption model		
		$q_m$ (mg/g)	$K_L$ (L/mg)	$R^2$
$\text{Hg}^{2+}$	843.6	909.1	0.3333	0.9992

**Table S4** Comparison of adsorption capacities of Hg<sup>2+</sup> ions by different MOFs adsorbents

<b>Materials</b>	<b>Adsorption capacity of Hg<sup>2+</sup> ions (mg/g)</b>	<b>Refs.</b>
PCN-224-MAA(O)	843.6	This work
PCN-222-MAA(O)	509.1	This work
ZIF-90-THP	596	7
ZIF-90-THF	403	7
Fe-BTC	210	8
Fe-BTC/PDA	1670	8
TMU-40	269	9
In <sub>2</sub> S <sub>3</sub> @MIL-101	518.2	10
Zr-DMBD	171.5	11
NH <sub>2</sub> -MIL-101(Al) MOF	124.8	12
Fe <sub>3</sub> O <sub>4</sub> @Cu <sub>3</sub> (btc) <sub>2</sub> -SH	158.23	5
JUC-62	836.7	13
UiO-66-NHC(S)NHMe	769	14
FJI-H12	439.8	15
MFC-S	282	16

## 5. References

1. D. Feng, Z. Y. Gu, J. R. Li, H. L. Jiang, Z. Wei and H. C. Zhou, *Angew. Chem. Int. Ed.*, 2012, **51**, 10307-10310.
2. H. Q. Xu, J. Hu, D. Wang, Z. Li, Q. Zhang, Y. Luo, S. H. Yu and H. L. Jiang, *J. Am. Chem. Soc.*, 2015, **137**, 13440-13443.
3. D. Feng, W. C. Chung, Z. Wei, Z. Y. Gu, H. L. Jiang, Y. P. Chen, D. J. Darensbourg and H. C. Zhou, *J. Am. Chem. Soc.*, 2013, **135**, 17105-17110.
4. L. Huang, M. He, B. Chen and B. Hu, *J. Mater. Chem. A*, 2015, **3**, 11587-11595.
5. F. Ke, J. Jiang, Y. Li, J. Liang, X. Wan and S. Ko, *Appl. Surf. Sci.*, 2017, **413**, 266-274.
6. Q. Sun, B. Aguila, J. Perman, L. D. Earl, C. W. Abney, Y. Cheng, H. Wei, N. Nguyen, L. Wojtas and S. Ma, *J. Am. Chem. Soc.*, 2017, **139**, 2786-2793.
7. W. H. Yin, Y. Y. Xiong, H. Q. Wu, Y. Tao, L. X. Yang, J. Q. Li, X. L. Tong and F. Luo, *Inorg. Chem.*, 2018, **57**, 8722-8725.
8. D. T. Sun, L. Peng, W. S. Reeder, S. M. Moosavi, D. Tiana, D. K. Britt, E. Oveisi and W. L. Queen, *ACS Cent. Sci.*, 2018, **4**, 349-356.
9. F. Rouhani and A. Morsali, *Chemistry*, 2018, **24**, 5529-5537.
10. L. Liang, L. Liu, F. Jiang, C. Liu, D. Yuan, Q. Chen, D. Wu, H. L. Jiang and M. Hong, *Inorg. Chem.*, 2018, **57**, 4891-4897.
11. L. Ding, X. Luo, P. Shao, J. Yang and D. Sun, *ACS Sustainable Chem. Eng.*, 2018, **6**, 8494-8502.
12. A. Shahat, S. A. Elsalam, J. M. Herrero-Martínez, E. F. Simó-Alfonso and G. Ramis-Ramos, *Sensors Actuat. B-Chem.*, 2017, **253**, 164-172.
13. Y. Wu, G. Xu, F. Wei, Q. Song, T. Tang, X. Wang and Q. Hu, *Microporous and Mesoporous Mater.*, 2016, **235**, 204-210.
14. H. Saleem, U. Rafique and R. P. Davies, *Microporous and Mesoporous Mater.*, 2016, **221**, 238-244.
15. L. Liang, Q. Chen, F. Jiang, D. Yuan, J. Qian, G. Lv, H. Xue, L. Liu, H.-L. Jiang and M. Hong, *J. Mater. Chem. A*, 2016, **4**, 15370-15374.
16. L. Huang, M. He, B. Chen and B. Hu, *J. Mater. Chem. A*, 2016, **4**, 5159-5166.